Network clique cover approximation to analyze complex contagions through group interactions

Supplementary Information

Giulio Burgio[1], Alex Arenas[1], Sergio Gómez[1], Joan T. Matamalas[2]

[1] Departament d'Enginyeria Informàtica i Matemàtiques,
Universitat Rovira i Virgili, 43007 Tarragona, Spain

[2] Center for Interdisciplinary Cardiovascular Sciences, Cardiovascular Division,
Department of Medicine, Brigham and Women's Hospital,
Harvard Medical School, Boston, MA 02115, USA

Contents

1 Robustness of MECLE under changes in the EECC 2
2 MECLE for simplicial 2-complexes 3
3 Epidemic threshold for highly symmetrical structures 6
4 Continuous-time limit of MECLE for simplicial 2-complexes 9
Supplementary References 12
Supplementary Figure 1: Robustness of MECLE on EECC for 0-connected SCs 13
Supplementary Figure 2: Robustness of MECLE on EECC for non-0-connected SCs 14
Supplementary Figure 3: Epidemic threshold for regular SCs 15
Supplementary Figure 4: Epidemic threshold for Friendship SCs 16
Supplementary Figure 5: Epidemic threshold for Dorogovtsev-Mendes SC in the continuous-time limit 17

Supplementary Note 1. Robustness of MECLE under changes in the EECC

Here we assess the dependence of the predictions made by the MECLE on the use of different EECCs found for a given SC $\mathcal{K}$. If the maximal cliques of the underlying graph $\mathcal{K}^{(1)}$ of the latter are all mutually edge-disjoint, then there is a unique EECC. Otherwise, two cases must be distinguished: (i) $\mathcal{K}$ is 0-connected, so the only non-edge-disjoint cliques in $\mathcal{K}^{(1)}$ are cliques also in $\mathcal{K}$ (i.e., they are $(0,\cdot)$-cliques); (ii) $\mathcal{K}$ is non-0-connected, so the non-edge-disjoint cliques in $\mathcal{K}^{(1)}$ can be either cliques or simplices in $\mathcal{K}$ (i.e., $(0,\cdot)$- or $(1,\cdot)$-cliques, respectively). The MECLE strictly applies only to the case (i) but, as shown in the main text, it keeps working well when the 0-connectedness is only slightly broken. In order to prove how robust is the MECLE in both cases, we consider structures possessing high proportions of edges shared by multiple cliques. Indeed, the higher is the number of times edges are shared, the higher is the probability that the proposed heuristic returns (proportionally) different EECCs. We recall that the algorithm is not deterministic only when, at some point, among the cliques with the minimum score, there are multiple ones having maximum order, among which one is randomly chosen (step 4(b) of the proposed heuristic).

Let us first focus on case (i). The best way to prove the robustness of the MECLE is, in this case, considering a graph (i.e., a simplicial 2-complex), so that the number of overlapping maximal $(0,\cdot)$-cliques is maximized; otherwise, some of them would be $(1,\cdot)$-cliques, which in this case are supposed 0-connected and hence not affecting the edge covering. In Supplementary Fig. 1 we show and discuss the results obtained computing several EECCs of a graph generated by the Dorogovtsev-Mendes model [1]. Such a graph has no tree-like portions. Despite its high rate of edge overlap, the prediction made by the MECLE is substantially independent from the used covering.

Going to case (ii), we consider several EECCs of the clique complex of the Dorogovtsev-Mendes network used in (i). The clique complex is obtained by converting all the 3-cliques of the network in 2-faces, so it is strongly non-0-connected. Note that the MECLE could be unreliable for such structure, since the algorithm destroys so many 2-faces that the resulting EECCs are too far from the original structure. The results in Supplementary Fig. 2 show the low variability among the EECCs provided by our heuristic and, consequently, among the predictions made by the MECLE, even for highly non-0-connected structures. Accordingly, such variability becomes negligible when the SC only slightly breaks the 0-connectedness condition, so that is sufficient to consider just one EECC. This is the case for the SCs considered in Fig. 5, for which the MECLE is still reliable.

Supplementary Note 2. MECLE for simplicial 2-complexes

We here illustrate the form taken by the MECLE model when the interaction structure is a simplicial 2-complex, i.e., the $(3,3)$ implementation of the model. Cliques and faces can only have order $n = 2, 3$.

The evolution of the probability P_i^I for node i being infected is governed by Eq. (8), which now takes the form

$$P_i^I\left(t+1\right) = P_i^I\left(t\right)\left(1-\mu\right) + P_i^S\left(t\right)\left(1 - q_{i,0}^{(1)} q_{i,0}^{(2)} q_{i,1}^{(2)}\right) \tag{S1}$$

where

$$q_{i,0}^{(1)} = \prod_{j\in\Gamma_{i,0}^{(1)}}\left[1-\beta^{(1)}P_{j|i,0}^{I|S}\right] \tag{S2a}$$

$$q_{i,g}^{(2)} = \prod_{\{j,k\}\in\Gamma_{i,g}^{(2)}}\left[1-\beta^{(1)}\left(P_{jk|i,g}^{IS|S}+P_{jk|i,g}^{SI|S}\right)-\left(1-\left(1-\beta^{(1)}\right)^2\left(1-g\beta^{(2)}\right)\right)P_{jk|i,g}^{II|S}\right] \tag{S2b}$$

According to Eq. (2), the state of a $(0,1)$-clique $\{i,j\}$ is governed by the following equations

$$\begin{aligned}
P_{ij,0}^{II}(t+1) &= P_{ij,0}^{SS}(t)\left(1-q_{i(j),0}^{(1)}q_{i,0}^{(2)}q_{i,1}^{(2)}\right)\left(1-q_{j(i),0}^{(1)}q_{j,0}^{(2)}q_{j,1}^{(2)}\right)\\
&+ P_{ij,0}^{SI}(t)\left(1-(1-\beta^{(1)})q_{i(j),0}^{(1)}q_{i,0}^{(2)}q_{i,1}^{(2)}\right)(1-\mu)\\
&+ P_{ij,0}^{IS}(t)\left(1-\mu\right)\left(1-(1-\beta^{(1)})q_{j(i),0}^{(1)}q_{j,0}^{(2)}q_{j,1}^{(2)}\right)\\
&+ P_{ij,0}^{II}(t)\left(1-\mu\right)^2
\end{aligned} \tag{S3a}$$

$$\begin{aligned}
P_{ij,0}^{IS}(t+1) &= P_{ij,0}^{SS}(t)\left(1-q_{i(j),0}^{(1)}q_{i,0}^{(2)}q_{i,1}^{(2)}\right)\left(q_{j(i),0}^{(1)}q_{j,0}^{(2)}q_{j,1}^{(2)}\right)\\
&+ P_{ij,0}^{SI}(t)\left(1-(1-\beta^{(1)})q_{i(j),0}^{(1)}q_{i,0}^{(2)}q_{i,1}^{(2)}\right)\mu\\
&+ P_{ij,0}^{IS}(t)\left(1-\mu\right)\left((1-\beta^{(1)})q_{j(i),0}^{(1)}q_{j,0}^{(2)}q_{j,1}^{(2)}\right)\\
&+ P_{ij,0}^{II}(t)\left(1-\mu\right)\mu
\end{aligned} \tag{S3b}$$

where $q_{i(j),0}^{(1)}$ coincides with $q_{i,0}^{(1)}$ except for excluding the $(0,1)$-clique $\{i,j\}$ from the product, and analogously for the other similar terms.

The state of a $(0,2)$-clique $\{i,j,k\}$ follows the equations

$$
\begin{aligned}
P^{III}_{ijk,0}(t+1) &= P^{SSS}_{ijk,0}(t)\left(1-q^{(1)}_{i,0}q^{(2)}_{i(jk),0}q^{(2)}_{i,1}\right)\left(1-q^{(1)}_{j,0}q^{(2)}_{j(ik),0}q^{(2)}_{j,1}\right)\left(1-q^{(1)}_{k,0}q^{(2)}_{k(ij),0}q^{(2)}_{k,1}\right)\\
&+ P^{SSI}_{ijk,0}(t)\left(1-\left(1-\beta^{(1)}\right)q^{(1)}_{i,0}q^{(2)}_{i(jk),0}q^{(2)}_{i,1}\right)\left(1-\left(1-\beta^{(1)}\right)q^{(1)}_{j,0}q^{(2)}_{j(ik),0}q^{(2)}_{j,1}\right)(1-\mu)\\
&+ P^{SIS}_{ijk,0}(t)\left(1-\left(1-\beta^{(1)}\right)q^{(1)}_{i,0}q^{(2)}_{i(jk),0}q^{(2)}_{i,1}\right)(1-\mu)\left(1-\left(1-\beta^{(1)}\right)q^{(1)}_{k,0}q^{(2)}_{k(ij),0}q^{(2)}_{k,1}\right)\\
&+ P^{ISS}_{ijk,0}(t)(1-\mu)\left(1-\left(1-\beta^{(1)}\right)q^{(1)}_{j,0}q^{(2)}_{j(ik),0}q^{(2)}_{j,1}\right)\left(1-\left(1-\beta^{(1)}\right)q^{(1)}_{k,0}q^{(2)}_{k(ij),0}q^{(2)}_{k,1}\right)\\
&+ P^{SII}_{ijk,0}(t)\left(1-\left(1-\beta^{(1)}\right)^2q^{(1)}_{i,0}q^{(2)}_{i(jk),0}q^{(2)}_{i,1}\right)(1-\mu)^2\\
&+ P^{ISI}_{ijk,0}(t)(1-\mu)\left(1-\left(1-\beta^{(1)}\right)^2q^{(1)}_{j,0}q^{(2)}_{j(ik),0}q^{(2)}_{j,1}\right)(1-\mu)\\
&+ P^{IIS}_{ijk,0}(t)(1-\mu)^2\left(1-\left(1-\beta^{(1)}\right)^2q^{(1)}_{k,0}q^{(2)}_{k(ij),0}q^{(2)}_{k,1}\right)\\
&+ P^{III}_{ijk,0}(t)(1-\mu)^3
\end{aligned}
\tag{S4a}
$$

$$
\begin{aligned}
P^{IIS}_{ijk,0}(t+1) &= P^{SSS}_{ijk,0}(t)\left(1-q^{(1)}_{i,0}q^{(2)}_{i(jk),0}q^{(2)}_{i,1}\right)\left(1-q^{(1)}_{j,0}q^{(2)}_{j(ik),0}q^{(2)}_{j,1}\right)\left(q^{(1)}_{k,0}q^{(2)}_{k(ij),0}q^{(2)}_{k,1}\right)\\
&+ P^{SSI}_{ijk,0}(t)\left(1-\left(1-\beta^{(1)}\right)q^{(1)}_{i,0}q^{(2)}_{i(jk),0}q^{(2)}_{i,1}\right)\left(1-\left(1-\beta^{(1)}\right)q^{(1)}_{j,0}q^{(2)}_{j(ik),0}q^{(2)}_{j,1}\right)\mu\\
&+ P^{SIS}_{ijk,0}(t)\left(1-\left(1-\beta^{(1)}\right)q^{(1)}_{i,0}q^{(2)}_{i(jk),0}q^{(2)}_{i,1}\right)(1-\mu)\left(\left(1-\beta^{(1)}\right)q^{(1)}_{k,0}q^{(2)}_{k(ij),0}q^{(2)}_{k,1}\right)\\
&+ P^{ISS}_{ijk,0}(t)(1-\mu)\left(1-\left(1-\beta^{(1)}\right)q^{(1)}_{j,0}q^{(2)}_{j(ik),0}q^{(2)}_{j,1}\right)\left(\left(1-\beta^{(1)}\right)q^{(1)}_{k,0}q^{(2)}_{k(ij),0}q^{(2)}_{k,1}\right)\\
&+ P^{SII}_{ijk,0}(t)\left(1-\left(1-\beta^{(1)}\right)^2q^{(1)}_{i,0}q^{(2)}_{i(jk),0}q^{(2)}_{i,1}\right)(1-\mu)\,\mu\\
&+ P^{ISI}_{ijk,0}(t)(1-\mu)\left(1-\left(1-\beta^{(1)}\right)^2q^{(1)}_{j,0}q^{(2)}_{j(ik),0}q^{(2)}_{j,1}\right)\mu\\
&+ P^{IIS}_{ijk,0}(t)(1-\mu)^2\left(\left(1-\beta^{(1)}\right)^2q^{(1)}_{k,0}q^{(2)}_{k(ij),0}q^{(2)}_{k,1}\right)\\
&+ P^{III}_{ijk,0}(t)(1-\mu)^2\,\mu
\end{aligned}
\tag{S4b}
$$

$$
\begin{aligned}
P^{ISS}_{ijk,0}(t+1) &= P^{SSS}_{ijk,0}(t)\left(1-q^{(1)}_{i,0}q^{(2)}_{i(jk),0}q^{(2)}_{i,1}\right)\left(q^{(1)}_{j,0}q^{(2)}_{j(ik),0}q^{(2)}_{j,1}\right)\left(q^{(1)}_{k,0}q^{(2)}_{k(ij),0}q^{(2)}_{k,1}\right)\\
&+ P^{SSI}_{ijk,0}(t)\left(1-\left(1-\beta^{(1)}\right)q^{(1)}_{i,0}q^{(2)}_{i(jk),0}q^{(2)}_{i,1}\right)\left(\left(1-\beta^{(1)}\right)q^{(1)}_{j,0}q^{(2)}_{j(ik),0}q^{(2)}_{j,1}\right)\mu\\
&+ P^{SIS}_{ijk,0}(t)\left(1-\left(1-\beta^{(1)}\right)q^{(1)}_{i,0}q^{(2)}_{i(jk),0}q^{(2)}_{i,1}\right)\mu\left(\left(1-\beta^{(1)}\right)q^{(1)}_{k,0}q^{(2)}_{k(ij),0}q^{(2)}_{k,1}\right)\\
&+ P^{ISS}_{ijk,0}(t)(1-\mu)\left(\left(1-\beta^{(1)}\right)q^{(1)}_{j,0}q^{(2)}_{j(ik),0}q^{(2)}_{j,1}\right)\left(\left(1-\beta^{(1)}\right)q^{(1)}_{k,0}q^{(2)}_{k(ij),0}q^{(2)}_{k,1}\right)\\
&+ P^{SII}_{ijk,0}(t)\left(1-\left(1-\beta^{(1)}\right)^2q^{(1)}_{i,0}q^{(2)}_{i(jk),0}q^{(2)}_{i,1}\right)\mu^2\\
&+ P^{ISI}_{ijk,0}(t)(1-\mu)\left(\left(1-\beta^{(1)}\right)^2q^{(1)}_{j,0}q^{(2)}_{j(ik),0}q^{(2)}_{j,1}\right)\mu\\
&+ P^{IIS}_{ijk,0}(t)(1-\mu)\,\mu\left(\left(1-\beta^{(1)}\right)^2q^{(1)}_{k,0}q^{(2)}_{k(ij),0}q^{(2)}_{k,1}\right)\\
&+ P^{III}_{ijk,0}(t)(1-\mu)\,\mu^2
\end{aligned}
\tag{S4c}
$$

where $q^{(2)}_{i(jk),0}$ coincides with $q^{(2)}_{i,0}$ except for excluding the $(0,2)$-clique $\{i,j,k\}$ from the product, and analogously for the other similar terms.

Finally, for a $(1,2)$-clique $\{i,j,k\}$, we get the following equations

$$
\begin{aligned}
P^{III}_{ijk,1}(t+1) = {} & P^{SSS}_{ijk,1}(t)\left(1-q^{(1)}_{i,0}q^{(2)}_{i,0}q^{(2)}_{i(jk),1}\right)\left(1-q^{(1)}_{j,0}q^{(2)}_{j,0}q^{(2)}_{j(ik),1}\right)\left(1-q^{(1)}_{k,0}q^{(2)}_{k,0}q^{(2)}_{k(ij),1}\right) \\
& + P^{SSI}_{ijk,1}(t)\left(1-\left(1-\beta^{(1)}\right)q^{(1)}_{i,0}q^{(2)}_{i,0}q^{(2)}_{i(jk),1}\right)\left(1-\left(1-\beta^{(1)}\right)q^{(1)}_{j,0}q^{(2)}_{j,0}q^{(2)}_{j(ik),1}\right)(1-\mu) \\
& + P^{SIS}_{ijk,1}(t)\left(1-\left(1-\beta^{(1)}\right)q^{(1)}_{i,0}q^{(2)}_{i,0}q^{(2)}_{i(jk),1}\right)(1-\mu)\left(1-\left(1-\beta^{(1)}\right)q^{(1)}_{k,0}q^{(2)}_{k,0}q^{(2)}_{k(ij),1}\right) \\
& + P^{ISS}_{ijk,1}(t)(1-\mu)\left(1-\left(1-\beta^{(1)}\right)q^{(1)}_{j,0}q^{(2)}_{j,0}q^{(2)}_{j(ik),1}\right)\left(1-\left(1-\beta^{(1)}\right)q^{(1)}_{k,0}q^{(2)}_{k,0}q^{(2)}_{k(ij),1}\right) \\
& + P^{SII}_{ijk,1}(t)\left(1-\left(1-\beta^{(1)}\right)^2\left(1-\beta^{(2)}\right)q^{(1)}_{i,0}q^{(2)}_{i,0}q^{(2)}_{i(jk),1}\right)(1-\mu)^2 \\
& + P^{ISI}_{ijk,1}(t)(1-\mu)\left(1-\left(1-\beta^{(1)}\right)^2\left(1-\beta^{(2)}\right)q^{(1)}_{j,0}q^{(2)}_{j,0}q^{(2)}_{j(ik),1}\right)(1-\mu) \\
& + P^{IIS}_{ijk,1}(t)(1-\mu)^2\left(1-\left(1-\beta^{(1)}\right)^2\left(1-\beta^{(2)}\right)q^{(1)}_{k,0}q^{(2)}_{k,0}q^{(2)}_{k(ij),1}\right) \\
& + P^{III}_{ijk,1}(t)(1-\mu)^3
\end{aligned}
\tag{S5a}
$$

$$
\begin{aligned}
P^{IIS}_{ijk,1}(t+1) = {} & P^{SSS}_{ijk,1}(t)\left(1-q^{(1)}_{i,0}q^{(2)}_{i,0}q^{(2)}_{i(jk),1}\right)\left(1-q^{(1)}_{j,0}q^{(2)}_{j,0}q^{(2)}_{j(ik),1}\right)\left(q^{(1)}_{k,0}q^{(2)}_{k,0}q^{(2)}_{k(ij),1}\right) \\
& + P^{SSI}_{ijk,1}(t)\left(1-\left(1-\beta^{(1)}\right)q^{(1)}_{i,0}q^{(2)}_{i,0}q^{(2)}_{i(jk),1}\right)\left(1-\left(1-\beta^{(1)}\right)q^{(1)}_{j,0}q^{(2)}_{j,0}q^{(2)}_{j(ik),1}\right)\mu \\
& + P^{SIS}_{ijk,1}(t)\left(1-\left(1-\beta^{(1)}\right)q^{(1)}_{i,0}q^{(2)}_{i,0}q^{(2)}_{i(jk),1}\right)(1-\mu)\left(\left(1-\beta^{(1)}\right)q^{(1)}_{k,0}q^{(2)}_{k,0}q^{(2)}_{k(ij),1}\right) \\
& + P^{ISS}_{ijk,1}(t)(1-\mu)\left(1-\left(1-\beta^{(1)}\right)q^{(1)}_{j,0}q^{(2)}_{j,0}q^{(2)}_{j(ik),1}\right)\left(\left(1-\beta^{(1)}\right)q^{(1)}_{k,0}q^{(2)}_{k,0}q^{(2)}_{k(ij),1}\right) \\
& + P^{SII}_{ijk,1}(t)\left(1-\left(1-\beta^{(1)}\right)^2\left(1-\beta^{(2)}\right)q^{(1)}_{i,0}q^{(2)}_{i,0}q^{(2)}_{i(jk),1}\right)(1-\mu)\,\mu \\
& + P^{ISI}_{ijk,1}(t)(1-\mu)\left(1-\left(1-\beta^{(1)}\right)^2\left(1-\beta^{(2)}\right)q^{(1)}_{j,0}q^{(2)}_{j,0}q^{(2)}_{j(ik),1}\right)\mu \\
& + P^{IIS}_{ijk,1}(t)(1-\mu)^2\left(\left(1-\beta^{(1)}\right)^2\left(1-\beta^{(2)}\right)q^{(1)}_{k,0}q^{(2)}_{k,0}q^{(2)}_{k(ij),1}\right) \\
& + P^{III}_{ijk,1}(t)(1-\mu)^2\,\mu
\end{aligned}
\tag{S5b}
$$

$$
\begin{aligned}
P^{ISS}_{ijk,1}(t+1) = {} & P^{SSS}_{ijk,1}(t)\left(1-q^{(1)}_{i,0}q^{(2)}_{i,0}q^{(2)}_{i(jk),1}\right)\left(q^{(1)}_{j,0}q^{(2)}_{j,0}q^{(2)}_{j(ik),1}\right)\left(q^{(1)}_{k,0}q^{(2)}_{k,0}q^{(2)}_{k(ij),1}\right) \\
& + P^{SSI}_{ijk,1}(t)\left(1-\left(1-\beta^{(1)}\right)q^{(1)}_{i,0}q^{(2)}_{i,0}q^{(2)}_{i(jk),1}\right)\left(\left(1-\beta^{(1)}\right)q^{(1)}_{j,0}q^{(2)}_{j,0}q^{(2)}_{j(ik),1}\right)\mu \\
& + P^{SIS}_{ijk,1}(t)\left(1-\left(1-\beta^{(1)}\right)q^{(1)}_{i,0}q^{(2)}_{i,0}q^{(2)}_{i(jk),1}\right)\mu\left(\left(1-\beta^{(1)}\right)q^{(1)}_{k,0}q^{(2)}_{k,0}q^{(2)}_{k(ij),1}\right) \\
& + P^{ISS}_{ijk,1}(t)(1-\mu)\left(\left(1-\beta^{(1)}\right)q^{(1)}_{j,0}q^{(2)}_{j,0}q^{(2)}_{j(ik),1}\right)\left(\left(1-\beta^{(1)}\right)q^{(1)}_{k,0}q^{(2)}_{k,0}q^{(2)}_{k(ij),1}\right) \\
& + P^{SII}_{ijk,1}(t)\left(1-\left(1-\beta^{(1)}\right)^2\left(1-\beta^{(2)}\right)q^{(1)}_{i,0}q^{(2)}_{i,0}q^{(2)}_{i(jk),1}\right)\mu^2 \\
& + P^{ISI}_{ijk,1}(t)(1-\mu)\left(\left(1-\beta^{(1)}\right)^2\left(1-\beta^{(2)}\right)q^{(1)}_{j,0}q^{(2)}_{j,0}q^{(2)}_{j(ik),1}\right)\mu \\
& + P^{IIS}_{ijk,1}(t)(1-\mu)\,\mu\left(\left(1-\beta^{(1)}\right)^2\left(1-\beta^{(2)}\right)q^{(1)}_{k,0}q^{(2)}_{k,0}q^{(2)}_{k(ij),1}\right) \\
& + P^{III}_{ijk,1}(t)(1-\mu)\,\mu^2
\end{aligned}
\tag{S5c}
$$

where $q^{(2)}_{i(jk),1}$ coincides with $q^{(2)}_{i,1}$ except for excluding the $(1,2)$-clique $\{i,j,k\}$ from the product, and analogously for the other similar terms.

Supplementary Note 3. Epidemic threshold for highly symmetrical structures

Given the high accuracy of the MECLE —as shown in the main text—, here we make further predictions for some particularly symmetrical structures, for which a closed form of $\beta_{\rm cr}^{(1)}$, expressing it in terms of the higher-order infection probabilities, $\{\beta^{(s)}\}_{s>1}$, and the recovery probability, μ, can be provided from Eq. (19). As a particular case, we show the monotonous decrease of $\beta_{\rm cr}^{(1)}$ with respect to $\beta^{(2)}$ in the herein examined 2-dimensional SCs. We stress that such dependence, as like as any other one, of $\beta_{\rm cr}^{(1)}$ on the higher-order couplings, is completely overlooked by models treating the nodes' states as uncorrelated.

Regular SCs. For a SC such that $k_i^{(g,r)} = k^{(g,r)}$, $\forall i \in V$, $\forall (g,r)$, since all the non-zero elements of M' are equal to the same constant, from the Collatz–Wielandt formula [2] it follows

$$\Lambda_{\max}\left(M'\right) = \sum_j M'_{ij} = \frac{\sum_{(g,r)} r k^{(g,r)} \sum_{l=1}^{r} \left(1 - w_{l,g}^{(r)}\right) \left[\binom{r-1}{l-1} X_{l,g}^{(r)} + \binom{r-1}{r-l-1} Y_{l,g}^{(r)}\right]}{\mu - \sum_{(g,r)} k^{(g,r)} \sum_{l=1}^{r} \binom{r}{l} \left(1 - w_{l,g}^{(r)}\right) Y_{l,g}^{(r)}} \tag{S6}$$

where both equalities hold for any chosen $i \in V$. Using Eq. (19), $\Lambda_{\max}\left(M'\right) = 1$, one can solve with respect to $\beta^{(1)}$ and express $\beta_{\rm cr}^{(1)}$ in terms of all the other parameters. The decreasing of $\beta_{\rm cr}^{(1)}$ with $\beta^{(2)}$ is shown in Supplementary Fig. 3 for two classes of regular simplicial 2-complexes. In particular, the periodic triangular clique complex, considered in the main text, falls within this class of structures. Note there is no dependence on the number of nodes, $N = |V|$.

Friendship SCs. As an opposite case, we consider now extremely heterogeneous SCs. A Friendship graph F_n is a Windmill graph $\mathrm{Wd}(m,n)$ whose "sails" are cliques of order $m = 3$. It consists of $N = 2n + 1$ nodes, where n is the number of 3-cliques incident on the central node. Starting from F_n, we convert a fraction $p_\triangle$ of the n 3-cliques in 2-faces. The central node has $k^{(0,2)} = (1 - p_\triangle)n \equiv n_0$ and $k^{(1,2)} = p_\triangle n \equiv n_1$. Then, $2n_0$ of the peripheral nodes have each $k^{(0,2)} = 1$ and $k^{(1,2)} = 0$, while the remaining $2n_1$ have $k^{(1,2)} = 1$ and $k^{(0,2)} = 0$. The greater N (hence, n), the higher the heterogeneity between the central node and the peripheral ones. In the large N limit, the average number of neighbors $\bar{k} = 3\frac{N-1}{N}$ tends to 3, whereas any higher m-moment diverges as N^{m-1}. Accordingly, we expect the epidemic threshold to vanish in that limit.

In order to find a closed expression for the epidemic threshold $\beta_{\rm cr}^{(1)}$, we take advantage of the nearly block structure featured by matrix M'. It can be partitioned as

$$M' = \begin{pmatrix} B & P \\ C & 0 \end{pmatrix} \tag{S7}$$

where B is a $(N-1) \times (N-1)$ block diagonal matrix, where each 2×2 block corresponds to the peripheral edge of a $(0,3)$- or a $(1,3)$-clique. That is, B can be put in the form

$$B = \mathrm{diag}(\underbrace{B_0, \ldots, B_0}_{n_0}, \underbrace{B_1, \ldots, B_1}_{n_1}) \tag{S8}$$

where

$$B_g = \begin{pmatrix} 0 & M'_{(P,g)} \\ M'_{(P,g)} & 0 \end{pmatrix} \tag{S9}$$

and

$$M'_{(P,g)} = \frac{\beta^{(1)}\left(X^{(2)}_{1,g} + Y^{(2)}_{1,g}\right) + \left(1 - \left(1-\beta^{(1)}\right)^2\left(1 - g\beta^{(2)}\right)\right) X^{(2)}_{2,g}}{\mu - 2\beta^{(1)} Y^{(2)}_{1,g} - \left(1 - \left(1-\beta^{(1)}\right)^2\left(1 - g\beta^{(2)}\right)\right) Y^{(2)}_{2,g}} \tag{S10}$$

for $g = 0, 1$. P is a $(N-1) \times 1$ matrix whose elements equal $M'_{(P,0)}$ or $M'_{(P,1)}$ depending on whether the peripheral node corresponding to the considered row participates, respectively, to a $(0,3)$- or a $(1,3)$-clique. Similarly, C is a $1 \times (N-1)$ matrix whose elements equal $M'_{(C,0)}$ or $M'_{(C,1)}$ depending on whether the central node participates, respectively, to a $(0,3)$- or a $(1,3)$-clique with the peripheral node corresponding to the considered column; where

$$M'_{(C,g)} = \frac{\beta^{(1)}\left(X^{(2)}_{1,g} + Y^{(2)}_{1,g}\right) + \left(1 - \left(1-\beta^{(1)}\right)^2\left(1 - g\beta^{(2)}\right)\right) X^{(2)}_{2,g}}{\mu - \sum_{g=0,1} n_g \left[2\beta^{(1)} Y^{(2)}_{1,g} + \left(1 - \left(1-\beta^{(1)}\right)^2\left(1 - g\beta^{(2)}\right)\right) Y^{(2)}_{2,g}\right]} \tag{S11}$$

for $g = 0, 1$.

We now compute the determinant of

$$M' - \lambda I_N = \begin{pmatrix} B - \lambda I_{N-1} & P \\ C & -\lambda \end{pmatrix} \tag{S12}$$

where I_N is the $N \times N$ identity matrix. Thanks to the Schur complement formula [2], we can compute it as

$$\det(M' - \lambda I_N) = \det(B - \lambda I_{N-1}) \left[-\lambda - C\left(B - \lambda I_{N-1}\right)^{-1} P\right] \tag{S13}$$

Using the properties of block diagonal matrices [2],

$$\det(B - \lambda I_{N-1}) = \left(\lambda^2 - {M'_{(P,0)}}^2\right)^{n_0} \left(\lambda^2 - {M'_{(P,1)}}^2\right)^{n_1} \tag{S14}$$

implying that $\lambda_{(P,g)} \equiv M'_{(P,g)}$, $\forall g \in \{0,1\}$, solves $\det(M' - \lambda I_N) = 0$; and therefore one between $\lambda_{(P,0)}$ and $\lambda_{(P,1)}$ is the leading eigenvalue of B. However, receiving contributions from peripheral nodes only, the latter can be shown to never coincide with the largest eigenvalue of M'. In particular, when both $n_0 > 1$ and $n_1 > 1$, we already know this is true, for the largest one is a simple eigenvalue [2]. Therefore, let us suppose $\lambda \neq \lambda_{(P,g)}$, $\forall g \in \{0,1\}$, and look for $\Lambda_{\max}(M')$ in the other factor, the one containing the contribution coming also from the central node. It is easily found that

$$\left(B - \lambda I_{N-1}\right)^{-1} = \mathrm{diag}(\underbrace{\tilde{B_0}^{-1}, \ldots, \tilde{B_0}^{-1}}_{n_0}, \underbrace{\tilde{B_1}^{-1}, \ldots, \tilde{B_1}^{-1}}_{n_1}) \tag{S15}$$

being

$$\tilde{B_g}^{-1} = \frac{1}{\lambda^2 - {M'_{(P,g)}}^2} \begin{pmatrix} -\lambda & -M'_{(P,g)} \\ -M'_{(P,g)} & -\lambda \end{pmatrix} \tag{S16}$$

the inverse matrix of $\tilde{B}_g = B_g - \lambda I_2$, $g = 0, 1$. With a few algebra, it follows

$$C\left(B - \lambda I_{N-1}\right)^{-1} P = -2\left(n_0 \frac{M'_{(P,0)} M'_{(C,0)}}{\lambda - M'_{(P,0)}} + n_1 \frac{M'_{(P,1)} M'_{(C,1)}}{\lambda - M'_{(P,1)}}\right) \tag{S17}$$

We now impose $\det(M' - \lambda I_N) = 0$ which, using the previous result $\lambda \neq \lambda_{(P,g)}$, $\forall g \in \{0,1\}$, reduces to $-\lambda - C\left(B - \lambda I_{N-1}\right)^{-1} P = 0$. This can be rearranged in the form

$$\lambda^3 - \lambda^2 \left(M'_{(P,0)} + M'_{(P,1)}\right) + \lambda \left(M'_{(P,0)} M'_{(P,1)} - 2n_0 M'_{(P,0)} M'_{(C,0)} - 2n_1 M'_{(P,1)} M'_{(C,1)}\right) + 2M'_{(P,0)} M'_{(P,1)} \left(n_0 M'_{(C,0)} + n_1 M'_{(C,1)}\right) = 0 \quad \text{(S18)}$$

We finally look for $\lambda = \Lambda_{\max}(M')$ among the solutions of Eq. (S18). As before, we solve $\Lambda_{\max}(M') = 1$ with respect to $\beta^{(1)}$ to find $\beta^{(1)}_{\text{cr}}$ as a function of the microscopic parameters, $\beta^{(2)}$ and μ, and of N and $p_{\triangle}$. Results are shown in Supplementary Fig. 4, where several values of N are explored for $p_{\triangle} = 0.5$. There is shown that the epidemic threshold vanishes in the limit of large N, while always decreasing with $\beta^{(2)}$. Interestingly, the dependence on $\beta^{(2)}$ grows with N, hence with the degree disparity between the central node and the peripheral ones. This, together with the weaker dependence found for regular structures (Supplementary Fig. 3), suggests that the dependence of $\beta^{(1)}_{\text{cr}}$ on $\beta^{(2)}$ grows with the heterogeneity of connections. In fact, as shown in Fig. 4, a very similar dependence is found for Dorogovtsev-Mendes SCs. This indicates that, despite their simplicity, the Friendship SCs are able to capture some important dynamical properties of more complex heterogeneous structures. To notice that, a strong correlation between edge-degree, $k^{(0,1)}$, and triangle-degree, $k^{(1,2)}$, of a node exists in both Dorogovtsev-Mendes SCs and Friendship SCs.

Supplementary Note 4. Continuous-time limit of MECLE for simplicial 2-complexes

It is possible to derive the continuous-time equations of the SIS dynamic in SCs as a limit of the MECLE model. Here, we show this process for the particular case of interaction structures arranged in simplicial 2-complexes, i.e., the continuous-time version of Eqs. S1-S5. In order to take the continuous-time limit, we make the substitutions

$$\mu \longrightarrow \mu\,\Delta t$$
$$\beta^{(s)} \longrightarrow \beta^{(s)}\,\Delta t$$

where now μ and $\beta^{(s)}$ represent rates, i.e., probabilities per unit time, instead of the original discrete-time probabilities [3]. Then, we take the limit $\Delta t \to 0$, which means neglecting all those terms in Eqs. S1-S5 appearing as second or greater powers of Δt or, equivalently, any combination of $\beta^{(1)}$, $\beta^{(2)}$ and μ. In other words, only single-node state changes are allowed during an infinitesimal interval dt.

The qs, Eqs. S2a-S2c, now become

$$q_{i,0}^{(1)} = 1 - \sum_{j\in\Gamma_{i,0}^{(1)}} \beta^{(1)} P_{j|i,0}^{I|S} \tag{S20a}$$

$$q_{i,g}^{(2)} = 1 - \sum_{\{j,k\}\in\Gamma_{i,g}^{(2)}} \left[\beta^{(1)}\left(P_{jk|i,g}^{IS|S} + P_{jk|i,g}^{SI|S} + 2P_{jk|i,g}^{II|S}\right) + g\beta^{(2)} P_{jk|i,g}^{II|S}\right] \tag{S20b}$$

from which the term $1 - q_{i,0}^{(1)} q_{i,0}^{(2)} q_{i,1}^{(2)}$, giving the probability that node i gets infected, reads

$$1 - q_{i,0}^{(1)} q_{i,0}^{(2)} q_{i,1}^{(2)} = \sum_{j\in\Gamma_{i,0}^{(1)}} \beta^{(1)} P_{j|i,0}^{I|S} + \sum_{g=0,1} \sum_{\{j,k\}\in\Gamma_{i,g}^{(2)}} \left[\beta^{(1)}\left(P_{jk|i,g}^{IS|S} + P_{jk|i,g}^{SI|S} + 2P_{jk|i,g}^{II|S}\right) + g\beta^{(2)} P_{jk|i,g}^{II|S}\right] \tag{S21}$$

The evolution of the probability P_i^I for node i being infected, now takes the form

$$\frac{d}{dt} P_i^I(t) = -\mu P_i^I(t) + P_i^S(t)\left(1 - q_{i,0}^{(1)} q_{i,0}^{(2)} q_{i,1}^{(2)}\right) \tag{S22}$$

where $1 - q_{i,0}^{(1)} q_{i,0}^{(2)} q_{i,1}^{(2)}$ is given by Eq. S21.

The state of a $(0,1)$-clique $\{i,j\}$ is governed by the following equations

$$\begin{aligned}\frac{d}{dt} P_{ij,0}^{II}(t) = {} & P_{ij,0}^{SI}(t)\left(\beta^{(1)} + 1 - q_{i(j),0}^{(1)} q_{i,0}^{(2)} q_{i,1}^{(2)}\right) \\ & + P_{ij,0}^{IS}(t)\left(\beta^{(1)} + 1 - q_{j(i),0}^{(1)} q_{j,0}^{(2)} q_{j,1}^{(2)}\right) \\ & - P_{ij,0}^{II}(t)\; 2\mu \end{aligned} \tag{S23a}$$

$$\begin{aligned}\frac{d}{dt} P_{ij,0}^{IS}(t) = {} & P_{ij,0}^{SS}(t)\left(1 - q_{i(j),0}^{(1)} q_{i,0}^{(2)} q_{i,1}^{(2)}\right) \\ & - P_{ij,0}^{IS}(t)\left(\mu + \beta^{(1)} + 1 - q_{j(i),0}^{(1)} q_{j,0}^{(2)} q_{j,1}^{(2)}\right) \\ & + P_{ij,0}^{II}(t)\; \mu \end{aligned} \tag{S23b}$$

where $q_{i(j),0}^{(1)}$ coincides with $q_{i,0}^{(1)}$ except for excluding the $(0,1)$-clique $\{i,j\}$ from the sum, and analogously for the other similar terms.

The state of a $(0,2)$-clique $\{i,j,k\}$ follows the equations

$$\begin{aligned}
\frac{d}{dt}P^{III}_{ijk,0}(t) &= P^{SII}_{ijk,0}(t)\left(2\beta^{(1)}+1-q^{(1)}_{i,0}q^{(2)}_{i(jk),0}q^{(2)}_{i,1}\right)\\
&+ P^{ISI}_{ijk,0}(t)\left(2\beta^{(1)}+1-q^{(1)}_{j,0}q^{(2)}_{j(ik),0}q^{(2)}_{j,1}\right)\\
&+ P^{IIS}_{ijk,0}(t)\left(2\beta^{(1)}+1-q^{(1)}_{k,0}q^{(2)}_{k(ij),0}q^{(2)}_{k,1}\right)\\
&- P^{III}_{ijk,0}(t)\ 3\mu \qquad \text{(S24a)}\\
\frac{d}{dt}P^{IIS}_{ijk,0}(t) &= P^{SIS}_{ijk,0}(t)\left(\beta^{(1)}+1-q^{(1)}_{i,0}q^{(2)}_{i(jk),0}q^{(2)}_{i,1}\right)\\
&+ P^{ISS}_{ijk,0}(t)\left(\beta^{(1)}+1-q^{(1)}_{j,0}q^{(2)}_{j(ik),0}q^{(2)}_{j,1}\right)\\
&- P^{IIS}_{ijk,0}(t)\left(2\mu+2\beta^{(1)}+1-q^{(1)}_{k,0}q^{(2)}_{k(ij),0}q^{(2)}_{k,1}\right)\\
&+ P^{III}_{ijk,0}(t)\ \mu \qquad \text{(S24b)}\\
\frac{d}{dt}P^{ISS}_{ijk,0}(t) &= P^{SSS}_{ijk,0}(t)\left(1-q^{(1)}_{i,0}q^{(2)}_{i(jk),0}q^{(2)}_{i,1}\right)\\
&- P^{ISS}_{ijk,0}(t)\left(\mu+2\beta^{(1)}+2-q^{(1)}_{j,0}q^{(2)}_{j(ik),0}q^{(2)}_{j,1}-q^{(1)}_{k,0}q^{(2)}_{k(ij),0}q^{(2)}_{k,1}\right)\\
&+ P^{ISI}_{ijk,0}(t)\ \mu\\
&+ P^{IIS}_{ijk,0}(t)\ \mu
\end{aligned}$$

where $q^{(2)}_{i(jk),0}$ coincides with $q^{(2)}_{i,0}$ except for excluding the $(0,2)$-clique $\{i,j,k\}$ from the sum, and analogously for the other similar terms.

Finally, for a $(1,2)$-clique $\{i,j,k\}$, we get the following equations

$$\begin{aligned}
\frac{d}{dt}P^{III}_{ijk,1}(t) &= P^{SII}_{ijk,1}(t)\left(2\beta^{(1)}+\beta^{(2)}+1-q^{(1)}_{i,0}q^{(2)}_{i,0}q^{(2)}_{i(jk),1}\right)\\
&+ P^{ISI}_{ijk,1}(t)\left(2\beta^{(1)}+\beta^{(2)}+1-q^{(1)}_{j,0}q^{(2)}_{j,0}q^{(2)}_{j(ik),1}\right)\\
&+ P^{IIS}_{ijk,1}(t)\left(2\beta^{(1)}+\beta^{(2)}+1-q^{(1)}_{k,0}q^{(2)}_{k,0}q^{(2)}_{k(ij),1}\right)\\
&- P^{III}_{ijk,1}(t)\ 3\mu \qquad \text{(S25a)}\\
\frac{d}{dt}P^{IIS}_{ijk,1}(t) &= P^{SIS}_{ijk,1}(t)\left(\beta^{(1)}+1-q^{(1)}_{i,0}q^{(2)}_{i,0}q^{(2)}_{i(jk),1}\right)\\
&+ P^{ISS}_{ijk,1}(t)\left(\beta^{(1)}+1-q^{(1)}_{j,0}q^{(2)}_{j,0}q^{(2)}_{j(ik),1}\right)\\
&- P^{IIS}_{ijk,1}(t)\left(2\mu+2\beta^{(1)}+\beta^{(2)}+1-q^{(1)}_{k,0}q^{(2)}_{k,0}q^{(2)}_{k(ij),1}\right)\\
&+ P^{III}_{ijk,1}(t)\ \mu \qquad \text{(S25b)}\\
\frac{d}{dt}P^{ISS}_{ijk,1}(t) &= P^{SSS}_{ijk,1}(t)\left(1-q^{(1)}_{i,0}q^{(2)}_{i,0}q^{(2)}_{i(jk),1}\right)\\
&- P^{ISS}_{ijk,1}(t)\left(\mu+2\beta^{(1)}+2-q^{(1)}_{j,0}q^{(2)}_{j,0}q^{(2)}_{j(ik),1}-q^{(1)}_{k,0}q^{(2)}_{k,0}q^{(2)}_{k(ij),1}\right)\\
&+ P^{ISI}_{ijk,1}(t)\ \mu\\
&+ P^{IIS}_{ijk,1}(t)\ \mu
\end{aligned}$$

where $q^{(2)}_{i(jk),1}$ coincides with $q^{(2)}_{i,1}$ except for excluding the $(1,2)$-clique $\{i,j,k\}$ from the sum, and analogously for the other similar terms.

Evidently, second-order dynamical correlations let $\beta^{(2)}$ appear in the dynamical equations. When linearizing Eqs. S20-S25 as done in Methods, the products between a state probability with some infected node and $1-q_{i,0}^{(1)}q_{i,0}^{(2)}q_{i,1}^{(2)}$ (et similia) disappear as negligible terms, while those ones corresponding to infections within the considered triangles do not. Consequently, $\beta^{(2)}$ does show up in the final eigenvalue equation providing the critical point, $\beta_{\rm cr}^{(1)}$. In Supplementary Fig. 5 we report the dependence of $\beta_{\rm cr}^{(1)}$ on $\beta^{(2)}$ as computed for a Dorogovtsev-Mendes SC.

Non-0-connected structures. Eq. S21 (or Eq. S20b) holds for a 0-connected SC. Nonetheless, differently from its discrete-time version, it can be adapted to hold for any connectedness. Indeed, the sum over the $(\cdot,3)$-cliques in Eq. S21 (or Eq. S20b) can now be split into two sums: one regarding the first-order infections coming from the edges of the $(\cdot,3)$-cliques, and one regarding the second-order infections coming from the $(1,3)$-cliques. In the former, rather than over the couples of neighbors of a node, one can sum over its single neighbors, in this way avoiding to over-count their contribution. To this end, one may define $\tilde{\Gamma}_i^{(2)}$ as the set of neighbors of node i such that $j\in\tilde{\Gamma}_i^{(2)}$ if $\exists k$ such that $\{j,k\}\in\Gamma_{i,g}^{(2)}$, $\forall g\in\{0,1\}$. Relaxing the edge-disjoint requirement, we can now look for a standard edge clique cover of the structure. Keeping the (g,n) nomenclature for the cliques in the cover, Eq. S21 adopts the form

$$1-q_{i,0}^{(1)}q_{i,0}^{(2)}q_{i,1}^{(2)}=\sum_{j\in\Gamma_{i,0}^{(1)}}\beta^{(1)}P_{j|i,0}^{I|S}+\sum_{j\in\tilde{\Gamma}_i^{(2)}}\beta^{(1)}\tilde{P}_{j|i}^{I|S}+\sum_{\{j,k\}\in\Gamma_{i,1}^{(2)}}\beta^{(2)}P_{jk|i,g}^{II|S} \tag{S26}$$

where $\tilde{P}_{j|i}^{I|S}\equiv P_{jk|i,g}^{II|S}+P_{jk|i,g}^{IS|S}$ for k such that $\{j,k\}\in\Gamma_{i,g}^{(2)}$. Since the edge $\{i,j\}$ is now allowed to be included in more than one $(\cdot,3)$-clique, k can identify more than one node. Differently from single nodes, a complete marginalization of the dynamical equation for the edge $\{i,j\}$, that would make $\tilde{P}_{j|i}^{I|S}$ independent from the chosen k, is however unfeasible (and not only with the chosen closure, Eq. (7)). Therefore, a more symmetrical way to evaluate $\tilde{P}_{j|i}^{I|S}$ is to compute it as the average value of $P_{jk|i,g}^{II|S}+P_{jk|i,g}^{IS|S}$ over all nodes k such that $\{j,k\}\in\Gamma_{i,g}^{(2)}$, $g=0,1$.

What has been done here for simplicial 2-complexes, can be extended to define the continuous-time limit of the MECLE for non-0-connected simplicial complexes of any higher dimension.

Supplementary References

[1] Dorogovtsev, S. N., Mendes, J. F. & Samukhin, A. N. Size-dependent degree distribution of a scale-free growing network. *Physical Review E* **63**, 062101 (2001).

[2] Meyer, C. D. *Matrix analysis and applied linear algebra*, vol. 71 (SIAM, 2000).

[3] Gómez, S., Gómez-Gardenes, J., Moreno, Y. & Arenas, A. Nonperturbative heterogeneous mean-field approach to epidemic spreading in complex networks. *Physical Review E* **84**, 036105 (2011).

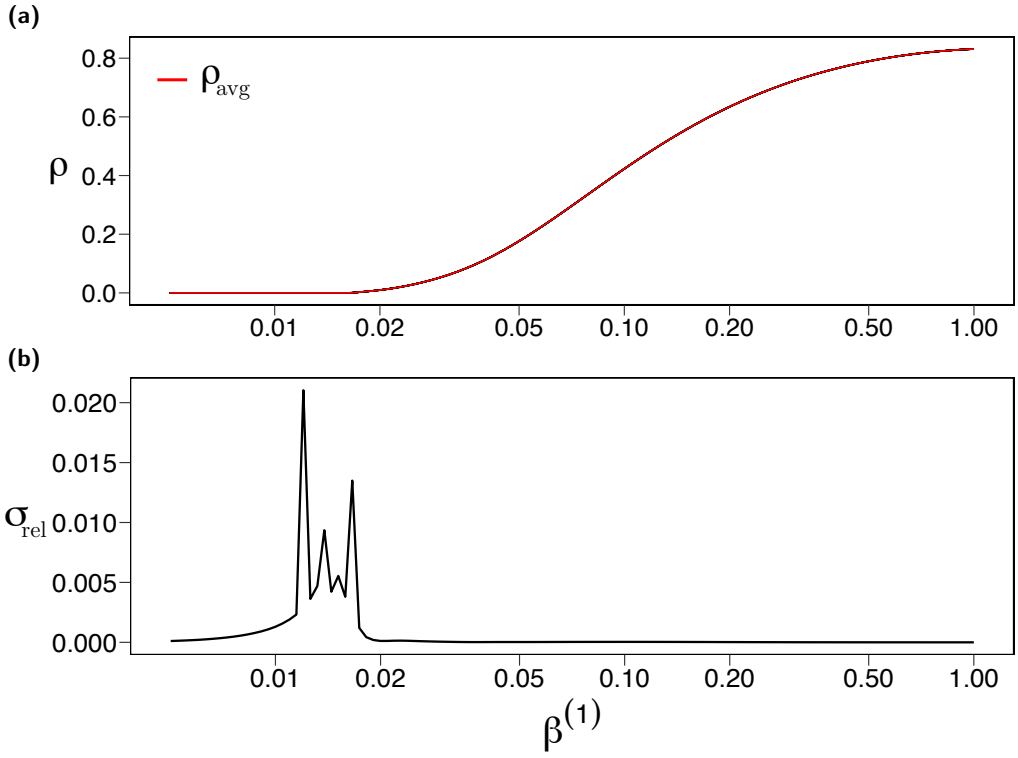

Supplementary Figure 1: The robustness of the MECLE under different EECCs is assessed for a graph generated from the Dorogovtsev-Mendes model, forming a 0-connected simplicial complex. This boasts a very high rate of edge overlap and, therefore, potentially different EECCs could lead the MECLE to make notably dissimilar predictions. Indeed, about 34% of the edges in the network are shared at least by two maximal cliques. Specifically, within that 34%, edges are shared by about 2.5 maximal cliques on average, with a standard deviation of 0.85 and a skewness of 2.3. The recovery probability is $\mu = 0.2$. (a) 20 prevalence curves obtained by 20 different EECCs are shown in black, while in red is reported their average curve $\rho_{\text{avg}}(\beta^{(1)})$, defined by the average value of ρ at each value of $\beta^{(1)}$. Since the deviations are below the width of the red line, the black lines are not visible. (b) The ratio σ_{rel} between the sample standard deviation σ and ρ_{avg} for each $\beta^{(1)}$. The value of σ_{rel} vanishes everywhere, expect for a small region around the epidemic threshold. This is below 2.5% for values of $\rho_{\text{avg}} \sim 10^{-4} \sim N^{-1}$, proving the remarkable robustness of the model.

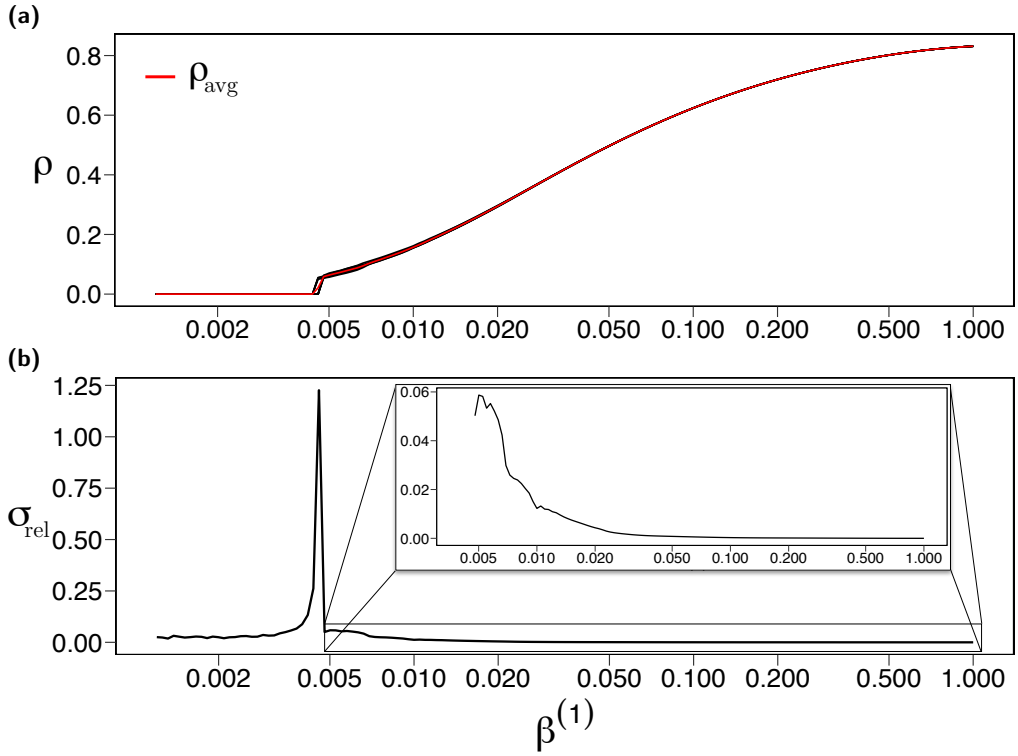

Supplementary Figure 2: The robustness of the MECLE under different EECCs is assessed for a non-0-connected simplicial complex generated from the Dorogovtsev-Mendes network used in Supplementary Fig. 1. The recovery probability is $\mu = 0.2$. (a) 20 prevalence curves obtained by 20 different EECCs are shown in black, while in red is reported their average curve $\rho_{\text{avg}}(\beta^{(1)})$, defined by the average value of ρ at each value of $\beta^{(1)}$. (b) The ratio σ_{rel} between the sample standard deviation σ and ρ_{avg} for each $\beta^{(1)}$. The pick at about $\beta^{(1)} = 0.0047$ is due to some curves transitioning at slightly different values of $\beta^{(1)}$. In fact, the uncertainty about the location of the critical point is of only about 0.0002, corresponding to a relative uncertainty of less than 5%. The inset plot shows a zoom of σ_{rel} to the right of the transition: σ_{rel} stays below the 6% next to the transition, while rapidly decreasing towards zero for larger $\beta^{(1)}$s, hence enlightening the robustness of the model.

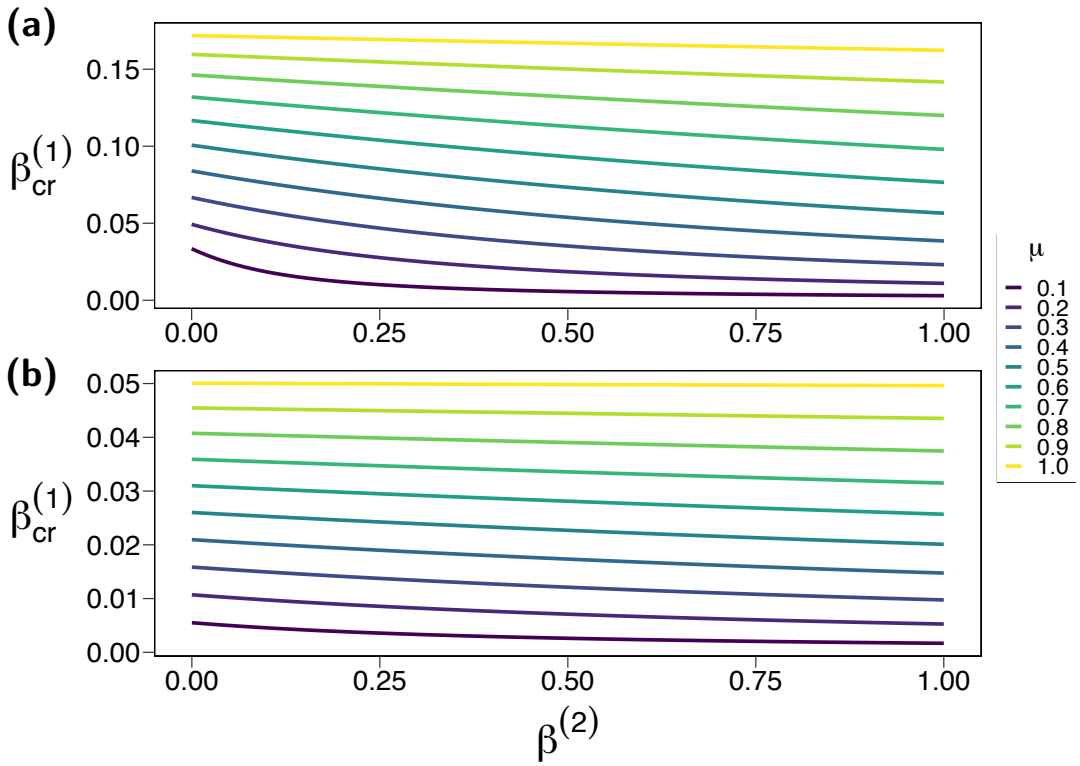

Supplementary Figure 3: The value of the epidemic threshold $\beta_{\rm cr}^{(1)}$, as computed from Eq. (S6), is shown against $\beta^{(2)}$ for (a) any regular clique 2-complex with $k^{(0,1)} = k^{(0)} = 0$ and $k^{(1,2)} = k^{(1)} = 3$ (the periodic triangular clique complex in the main text falls within this class); (b) any regular clique 2-complex with $k^{(0,1)} = k^{(0)} = 12$ and $k^{(1,2)} = k^{(1)} = 4$ (a proxy for large random SCs). Note that the mean-field approximation, Eq. (22), wrongly predicts $\beta_{\rm cr}^{(1)} = \mu/k$, $\forall \beta^{(2)}$, where $k = 6$ in (a), $k = 20$ in (b).

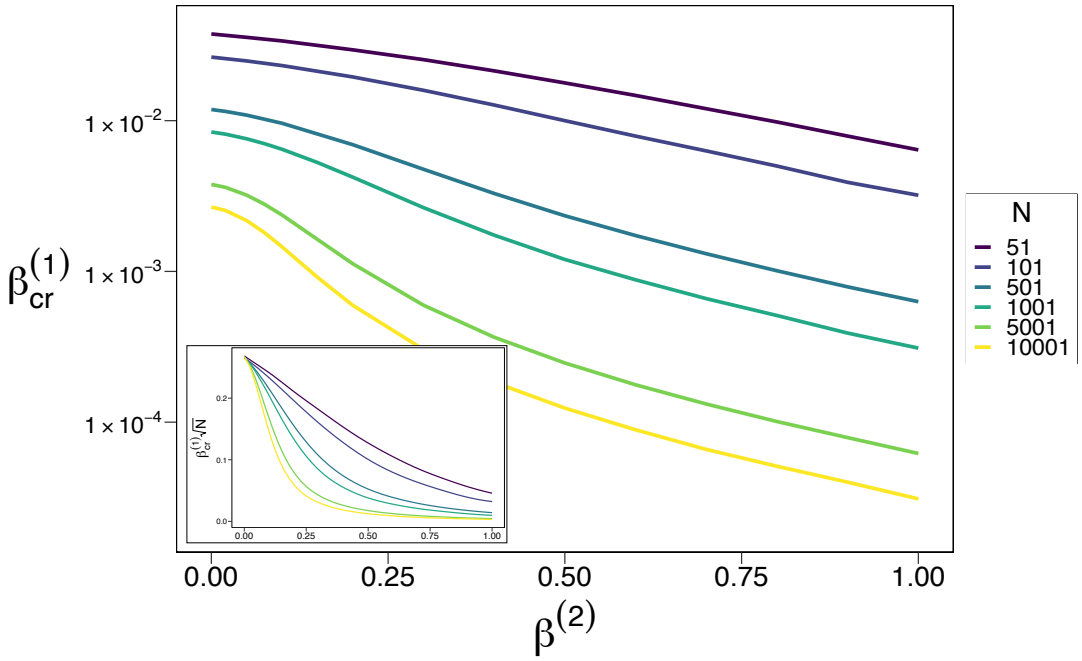

Supplementary Figure 4: The value of the epidemic threshold $\beta_{\rm cr}^{(1)}$ is shown against $\beta^{(2)}$ for simplicial 2-complexes constructed from the Friendship graph F_n, a proxy for extremely heterogeneous structures, where $n = \frac{N-1}{2}$. Here $p_\triangle = 0.5$, thus $k^{(0,2)} = k^{(1,2)} = n/2$ for the central node, $k^{(1,2)} = 1$ and $k^{(0,2)} = 0$ for half of the peripheral nodes, and $k^{(0,2)} = 0$ and $k^{(1,2)} = 1$ for the other half. The recovery probability is $\mu = 0.2$. The mean-field approximation, Eq. (22), wrongly predicts $\beta_{\rm cr}^{(1)} = \mu/\bar{k}$, $\forall \beta^{(2)}$, where $\bar{k} = 3\frac{N-1}{N}$. The inset plot shows the curves $\beta_{\rm cr}^{(1)}\sqrt{N}$ vs. $\beta^{(2)}$. These all collapse to the same value $x^* \approx 0.27$ at $\beta^{(2)} = 0$, while being smaller than x^* for any $\beta^{(2)} > 0$, hence proving that $\beta_{\rm cr}^{(1)} \to 0$ for $N \to \infty$, $\forall \beta^{(2)}$.

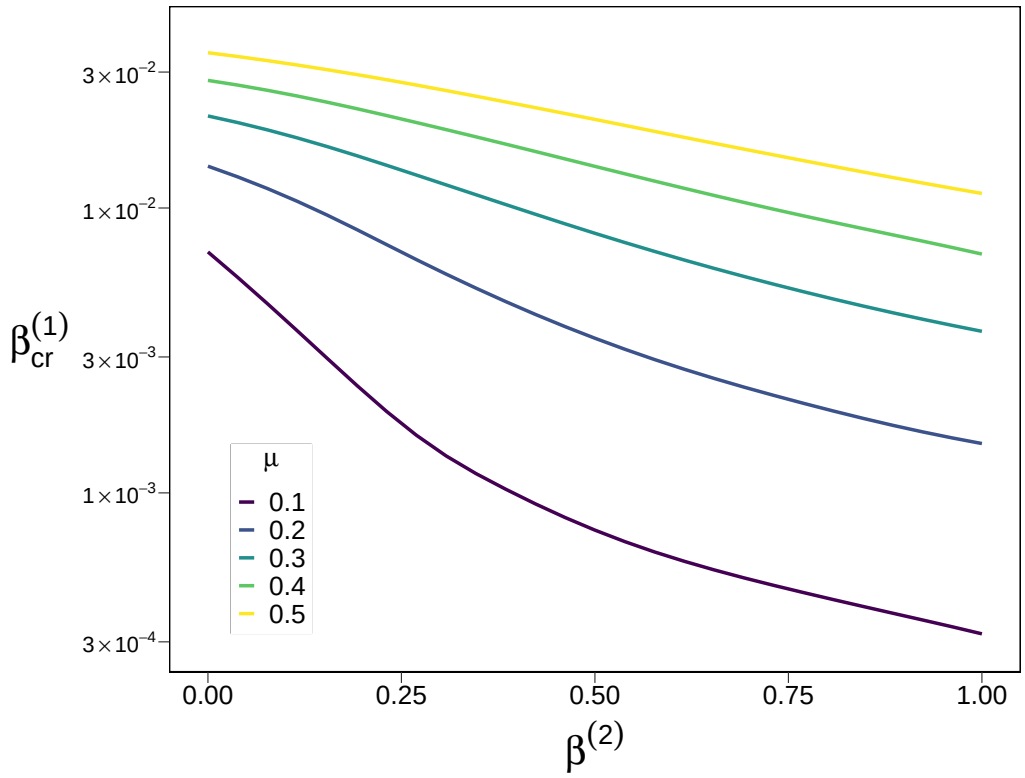

Supplementary Figure 5: The value of the epidemic threshold $\beta_{\rm cr}^{(1)}$, as predicted in the continuous-time limit by the MECLE, is shown against $\beta^{(2)}$ for a Dorogovtsev-Mendes SC with $\bar{k}^{(0,1)} = 1.10$ and $\bar{k}^{(1,2)} = 1.45$. The mean-field approximation, Eq. (22), wrongly predicts $\beta_{\rm cr}^{(1)} = \mu/\bar{k} = 0.05$, $\forall\beta^{(2)}$.